2018 5th International Workshop on Compressed Sensing applied to Radar, Multimodal Sensing, and Imaging (CoSeRa)

Analysis of Initial Estimate Noise in the Sparse Randomly Sampled ISAR Signals

L. Stanković[1], M. Brajović[1], I. Stanković[1,2], C. Ioana[2], M. Daković[1]
[1] Faculty of Electrical Engineering, University of Montenegro, 81000 Podgorica, Montenegro
[2] GIPSA Lab, Grenoble INP, Université Grenoble Alpes, 38000 Grenoble, France

***Abstract*—The variance calculation of the initial DFT estimate for a nonuniformly sampled signal in ISAR with a reduced set of samples is derived and statistically verified. The results for subsets of uniformly and randomly sampled signals follow as the special cases. The obtained results can be used to define an efficient threshold for the matching pursuit reconstruction and to derive the error in the final ISAR signal reconstruction using a reduced set of randomly positioned samples when the sparsity condition is not satisfied.**

***Index Terms*—ISAR, Compressive sensing, DFT, Sparse signals, Signal reconstruction**

I. Introduction

A radar image is obtained by calculating the two-dimensional Fourier transform (FT) of the received signal. The radar image consists of peaks of scattering points at the positions defined by the targets' range and cross-range. The images obtained using the transform of the received signals are called the inverse synthetic aperture radar (ISAR) images.

Having only few scattering points of the target, an ISAR image is considered as a sparse signal. That means that it has a small number of nonzero valued samples in comparison to the total length of the received signal. According to the theory of sparse signal processing and compressive sensing (CS) [1]–[3], a sparse signal can be reconstructed from much fewer samples than the sampling theorem requires. The set of available samples can be reduced for a number of reasons. Randomly positioned samples could be the result from heavily corrupted parts of the signal. These parts are then omitted and declared as unavailable, before the ISAR image recovery is done. Measurements and physical constraints of the target and radar interferences may also cause that only a small number of the randomly positioned data is received and measured. It can also be that the technique of sparse signal processing is applied and a reduced set of data is used. The application of the sparse signal processing and CS theory to the ISAR images was studied in recent years [4]–[11].

In this paper, the case of nonuniformly positioned available samples is considered. As it is common in the ISAR we will consider only the Doppler part of the signal. Since this part of the received signal will be considered, it means that the received chirps are available at nonuniform positions. There are two sources of randomness in the initial estimate. The first one is the lack of synchronization, causing random shift in sampling positions. The second one is that only a random subset of the full set of samples is available. The special cases when the positions are uniformly and randomly positioned are examined in [12]–[21]. In this paper, we will generalize the formula for the variance of the initial estimate, analytically defining the transition from the uniform to the random sampling. The theory will be verified on numerical examples.

The paper is organized as follows. After the introduction in Section I, the model of the signal with some basic definitions is presented in Section II. The idea of reduced set of measurements is explained in Section III, along with theoretical analysis of the initial estimate variance. Examples are shown in Section IV. The conclusions are presented in Section V.

II. Signal Model and Basic Definitions

The Doppler part of the received signal, after the distance compensation, from the l-th scattering point is

$$x_l(t) = A_l e^{j2\pi\omega_l t}, \tag{1}$$

where $\omega_l = 2\Omega_0 y_{l0}\omega_R T_r/c$ is the constant (frequency of the received signal) proportional to the velocity (cross-range y_{l0}) and t is the slow-time. The variables Ω_0, ω_R, T_r represent the radar operating angular frequency, carrier frequency and the single-chirp repetition time, respectively. Assuming K scattering points the total received signal is

$$x(t) = \sum_{l=1}^{K} x_l(t). \tag{2}$$

Observe the case when the chirps are transmitted or received at nonuniform instants $t_n = n + \nu_n$ with $0 \le n \le N-1$. In that case, the sampling of the Doppler part of received signal $x(t_n)$ will be nonuniform. The instants $t_n = n$ correspond to the discrete time values obtained in accordance with the sampling theorem, and ν_n is a random variable with a uniform distribution, where $-\Delta/2 \le \nu_n \le \Delta/2$. The variable ν_n is a random shift (caused intentionally or by the lack of synchronization). Without loss of generality, we have assumed a normalized sampling step in the sampling theorem $\Delta t = 1$. Two special cases of this among are the uniform sampling for $\Delta = 0$ and the random sampling for a large Δ. We will assume that a complete form of the signal has N samples. If the received signal is a K-component signal, with frequencies ω_l on a sampling grid, then it assumes the following analytical form

$$x(t_n) = \sum_{l=1}^{K} A_l e^{\frac{j2\pi}{N}k_l t_n}, \tag{3}$$

for $k_l \in \{0, 1, \ldots, N-1\}$. The discrete calculation requires integer indices. It means that only the target at the grid will have a sparse nature. However, this is not satisfied. Even one point reflector on an off-grid point then have nonzero values over the whole grid of integer points in the range/cross-range domain and the signal becomes nonsparse. The goal is to calculate the DFT of this signal using a reduced set of nonuniformly sampled signal values.

III. Reduced Set of Measurements

Assume that a reduced set of M random signal samples (measurements) is available, where $M \leq N$. If the full set of time instants is denoted by $\mathbf{\Lambda} = \{t_0, t_1, \ldots, t_{N-1}\}$, then the subset of time instants where the measurements are available is $\mathbf{\Omega} = \{t_{n_1}, t_{n_2}, ..., t_{n_M}\} \subseteq \mathbf{\Lambda}$. Since the random set of available samples is used, the subset of positions t_{n_i} is random. Observe that

$$n_i \in \mathbf{M}_A = \{n_1, n_2, \ldots, n_M\},$$

where $\mathbf{M}_A \subseteq \mathbf{N} = \{0, 1, \ldots, N-1\}$. In the case of a reduced set of samples, the signal can be written in the form of measurements (within the compressive sensing notation) as

$$\mathbf{y} = \mathbf{A}\mathbf{X} \tag{4}$$

where the available signal samples at $\mathbf{\Omega} = \{t_{n_1}, t_{n_2}, ..., t_{n_M}\}$ are denoted by

$$\mathbf{y} = [x(t_1)\ x(t_2) \ldots x(t_M)]^T. \tag{5}$$

The elements of the measurement matrix $\mathbf{A}$ are

$$a(n_i, k) = e^{\frac{j2\pi}{N} k t_{n_i}} \tag{6}$$

for $i = 1, 2, \ldots, M$ and $k = 0, 1, \ldots, N-1$. The initial estimate in the reconstruction algorithms plays a crucial role, and, in general, it determines the reconstruction efficiency in an implicit way. The initial DFT estimate is obtained as

$$\mathbf{X}_0 = \mathbf{A}^H \mathbf{y}. \tag{7}$$

The initial estimate of the DFT coefficients of the signal $x(t_n)$ can be written as

$$X_0(k) = \sum_{n \in \mathbf{M}_A} x(t_n) e^{-j\frac{2\pi}{N} t_n k}. \tag{8}$$

For a random set of instants where the signal is available and random deviation of the instants, the coefficients $X_0(k)$ are random variables [21]. Properties of these random variables are crucial in the reconstruction.

A. Monocomponent signal

Aiming to calculate the basic parameters of the initial DFT coefficients as random variables, first we observe a one-component signal, i.e. $K = 1$, with amplitude A_1 and frequency k_1. The initial DFT of this signal reads

$$\begin{aligned} X_0(k) &= \sum_{n \in \mathbf{M}_A} A_1 e^{j\frac{2\pi}{N}(k-k_1)t_n} \\ &= \sum_{n \in \mathbf{M}_A} A_1 e^{j\frac{2\pi}{N}(k-k_1)n} e^{j\frac{2\pi}{N}(k-k_1)\nu_n}. \end{aligned} \tag{9}$$

We will determine the mean value $\mu_{X_0(k)}$ and the variance $\sigma^2_{X_0(k)}$ of the DFT coefficient acting as a random variable. The mean value is

$$\mu_{X_0(k)} = A_1 \sum_{n \in \mathbf{M}_A} E\{e^{j\frac{2\pi}{N}(k-k_1)n}\} E\{e^{j\frac{2\pi}{N}(k-k_1)\nu_n}\}. \tag{10}$$

It is easy to show [16] that

$$E\{e^{j\frac{2\pi}{N}(k-k_1)n}\} = \delta(k-k_1), \tag{11}$$

where $\delta(k-k_1) = 1$ for $k = k_1$ and $\delta(k-k_1) = 0$ for $k \neq k_1$.

Now we will observe the term

$$\mu_\nu = E\{e^{j\frac{2\pi}{N}(k-k_1)\nu_n}\}.$$

According to the definition of the expected value we get

$$\begin{aligned} \mu_\nu &= \int_{-\Delta/2}^{\Delta/2} p(\Theta) e^{j\frac{2\pi}{N}(k-k_1)\Theta} d\Theta \\ &= \frac{\sin\left(\frac{\pi(k-k_1)\Delta}{N}\right)}{\frac{\pi(k-k_1)\Delta}{N}} = \mathrm{sinc}\left(\frac{\pi(k-k_1)\Delta}{N}\right), \end{aligned} \tag{12}$$

where the probability density function $p(\Theta) = \frac{1}{\Delta}$ is used for the uniform random variable $\Theta = \nu_n$ within the interval $[-\frac{\Delta}{2}, \frac{\Delta}{2}]$. This result will be used in the derivation of the variance. For $k = k_1$, we get $\mu_\nu = 1$.

For M terms in (10), we get

$$\mu_{X_0(k)} = A_1 M \delta(k-k_1). \tag{13}$$

In order to determine the variance of $X_0(k)$, the analysis will be conducted for two possible cases: $k \neq k_1$ and $k = k_1$.

- For $k \neq k_1$, the mean value of the DFT coefficient is equal to zero, i.e. $\mu_{X_0(k)} = 0$. In that case, the variance is calculated by definition as

$$\begin{aligned} \sigma^2_{X_0(k)} = \sum_{n \in \mathbf{M}_A} \sum_{m \in \mathbf{M}_A} |A_1|^2 E\{e^{j\frac{2\pi}{N}(k-k_1)(n-m)}\} \\ \times E\{e^{j\frac{2\pi}{N}(k-k_1)(\nu_n-\nu_m)}\}. \end{aligned} \tag{14}$$

  For the second expected value appearing in (14) and for $n \neq m$, we obtain

$$E\{e^{j\frac{2\pi}{N}(k-k_1)(\nu_n-\nu_m)}\} = E\{e^{j\frac{2\pi}{N}k_1\nu_n}\} E\{e^{j\frac{2\pi}{N}k\nu_m}\} = \mu_\nu^2$$

  as expectations over ν_n and ν_m are independent ($k \neq k_1$). For $n = m$, the analyzed expectation becomes

$$E\{e^{j\frac{2\pi}{N}(k-k_1)(\nu_n-\nu_m)}\} = 1.$$

  It has been previously established in [16] that for random $n \neq m$ and $k \neq k_1$ variables $e^{j\frac{2\pi}{N}(k-k_1)n}$ are equally distributed, producing expectation

$$E\{e^{j\frac{2\pi}{N}(k-k_1)(n-m)}\} = -\frac{1}{N-1}. \tag{15}$$

  Otherwise, for $n = m$, the complex sinusoid is deterministic, and relation $E\{e^{j\frac{2\pi}{N}(k-k_1)(n-m)}\} = 1$ holds.

In (14), there are M terms when $m = n$ and $M(M-1)$ terms for $m \neq n$. Therefore, for $k \neq k_1$ the DFT coefficient variance becomes

$$\sigma^2_{X_0(k)} = |A_1|^2 M\left[1 - \frac{M-1}{N-1}\mathrm{sinc}^2\left(\frac{\pi(k-k_1)\Delta}{N}\right)\right]. \tag{16}$$

As it is expected, for $\Delta \to 0$ the term

$$\mathrm{sinc}\left(\frac{\pi(k-k_1)\Delta}{N}\right) = \frac{\sin(\frac{\pi(k-k_1)\Delta}{N})}{\pi(k-k_1)\Delta/N} \to 1,$$

leading to

$$\sigma^2_{X_0(k)} = |A_1|^2 \frac{M(N-M)}{N-1}.$$

This is the variance for the initial estimate with a reduced set of samples on the uniform discrete time grid [16]. Moreover, for a large Δ, such that the second term in the variance can be neglected, we get the other special case of fully random signal sampling [21]

$$\sigma^2_{X_0(k)} = |A_1|^2 M.$$

In general, the variance is dependent on frequency. The average value of the variance can be used as an frequency independent estimate. It depends on the parameter

$$S(\Delta) = \frac{1}{N}\sum_{k=1}^{N}\mathrm{sinc}^2\left(\frac{\pi k\Delta}{N}\right).$$

The value of this variance parameter cannot be calculated analytically. Its value for various Δ (or Δ/N) is shown in Fig. 1. The average value of variance is then

$$\overline{\sigma^2_{X_0(k)}} = |A_1|^2 M\big[1 - \frac{M-1}{N-1}S(\Delta)\big]. \tag{17}$$

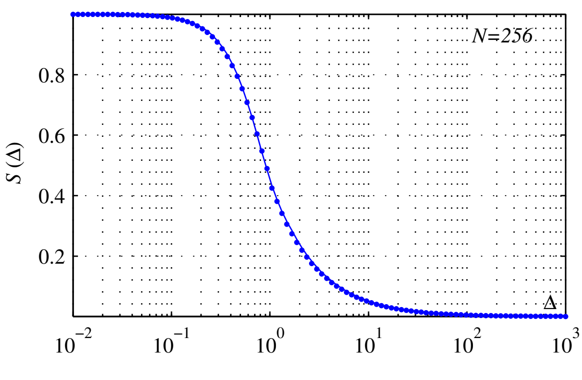

Fig. 1. Variance prameter $S(\Delta)$ for $N = 256$ and various Δ.

Very simple heuristic expressions can be used for approximation of $S(\Delta)$ as $S(\Delta) = 1/(1 + 1.2\Delta^2)$ for $\Delta < 1$ and $S(\Delta) = 1/(1+2\Delta)+1/(1+8\Delta^2)$ otherwise, shown in dots in Fig. 1 for $N = 256$.

- For the second considered case, when $k = k_1$, it is easy to obtain that

$$\sigma^2_{X_0(k)} = 0.$$

The general result for the variance for any frequency index k is

$$\sigma^2_{X_0(k)} = |A_1|^2 M\left[1 - \frac{M-1}{N-1}\mathrm{sinc}^2\left(\frac{\pi(k-k_1)\Delta}{N}\right)\right] \times \big[1 - \delta(k-k_1)\big]. \tag{18}$$

Observe that mean value and variances depend on $k - k_1$. It is interesting to note that the variance is a function of $(k - k_1)\Delta$. This observation will be confirmed by numerical results.

B. Multicomponent signals

In the case of K-component signals, the observed random variable is

$$X_0(k) = \sum_{n\in\mathbf{M}_A}\sum_{l=1}^{K} A_l e^{j\frac{2\pi}{N}(k-k_l)n} e^{j\frac{2\pi}{N}(k-k_l)\nu_n}. \tag{19}$$

This is a summation of independent random variables. Therefore, using (13), the mean value of the random variable $X(k)$ takes the following form:

$$\mu_{X_0(k)} = \sum_{l=1}^{K} A_l M\delta(k-k_l). \tag{20}$$

The variance of the DFT coefficients at positions $k \neq k_l, l \neq 1,\dots,K$, has the form of a sum of variances (16)

$$\sigma^2_{X_0(k)} = \sum_{l=1}^{K} M|A_l|^2\left[1 - \frac{M-1}{N-1}\mathrm{sinc}^2\left(\frac{\pi(k-k_l)\Delta}{N}\right)\right] \tag{21}$$

since the missing samples from each signal component contribute to the noise. These noises are uncorrelated, with zero mean and variances defined by (16).

For the DFT coefficient at a signal component position $k = k_p$, $p = 1,\dots K$, the missing samples in the pth signal component do not contribute to the resulting variance. However, remaining $K-1$ components at positions $k = k_l$, $l \neq p$, $l = 1,\dots,K$ contribute to the resulting initial estimate noise at $k = k_p$. Their variances are defined by (16). Therefore, the resulting variance at a signal component position $k = k_p$, $p = 1,\dots K$ is

$$\sigma^2_{X_0(k)} = \sum_{\substack{l=1\\ l\neq p}}^{K} M|A_l|^2\left[1 - \frac{M-1}{N-1}\mathrm{sinc}^2\left(\frac{\pi(k-k_l)\Delta}{N}\right)\right]. \tag{22}$$

The average value of this variance is

$$\sigma^2_{X_0(k)} = \sum_{\substack{l=1\\ l\neq p}}^{K} M|A_l|^2\left[1 - \frac{M-1}{N-1}S(\Delta)\right]. \tag{23}$$

It is frequency invariant.

IV. Numerical results

The obtained theoretical expressions for variances of DFT coefficients are next verified numerically.

First, we check a monocomponent signal on a frequency k_1. The theoretical and statistical results for $k_1 - k = 65, 75, 100, 155, 200,$ and 255 are presented in Fig. 2. The numerical results for variances are obtained based on 2000 independent realizations of signals samples available at instants from set $\mathbf{\Omega} = \{t_{n_1}, t_{n_2}, ..., t_{n_M}\}$ with random $n_i \in \mathbf{M}_A$, and random deviations $-\Delta/2 \le \nu_n \le \Delta/2$. The results are averaged over realizations for each considered value of parameter Δ. In all experiments, Fig. 2 (a)-(f) parameter Δ was varied from 0 to 4 with step 0.2. We can see that the diagrams are scaled version of each other along the Δ-axis. Since the variances are functions of $(k_1 - k)\Delta$ obviously the values in Fig. 2(c) for $0 \le \Delta \le 4$ correspond to the values in Fig. 2(e) for $0 \le \Delta \le 2$. The results in Fig. 2 are shown for four different values of available samples M.

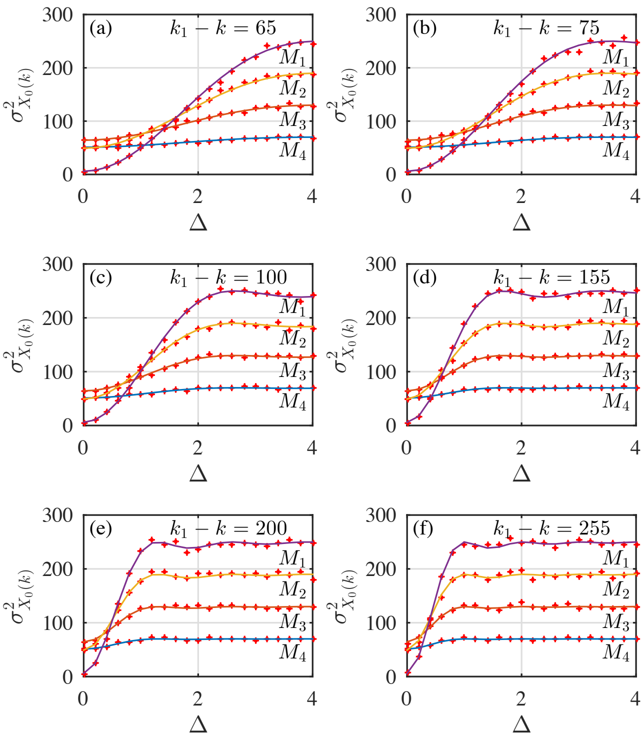

Fig. 2. Variance of the DFT coefficient at position $k = 3, k \neq k_1$ acting as a random variable in the case of signal with $M = M_i$, $i = 1, 2, 3, 4$ samples available at $t_n = n_i + \nu_n$, where $-\frac{\Delta}{2} \le \nu_n \le \frac{\Delta}{2}$. Variances are shown as functions of Δ. Four values of M are considered: $M_1 = 70$, $M_2 = 130$, $M_3 = 190$ and $M_4 = 250$. Results are shown for various k_1, (a)-(f). Lines represent theoretical values, whereas asterisks correspond to the numerical results.

Graphs of the variances as a function of $k_1 - k$, for three different values of $\Delta = 0.1, 5, 30$ and $M = 25, 150, 200$ are presented in Fig. 3. In this experiment, the numerical results are obtained averaging the results for 12000 independent realizations of signals with randomly positioned samples at $t_i \in \mathbf{\Omega}$, $i = 1, ..., M$.

Finally, a three-component signal

$$x(t_n) = \sum_{l=1}^{3} A_l e^{\frac{j2\pi}{N} k_l t_n}, \tag{24}$$

with $k_1 = 15$, $k_2 = 63$, and $k_3 = 192$ and unity amplitudes is considered. Its theoretical and statistical variances as functions of k are presented in Fig. 4.

In all cases the agreement between the theory and statistics is very high.

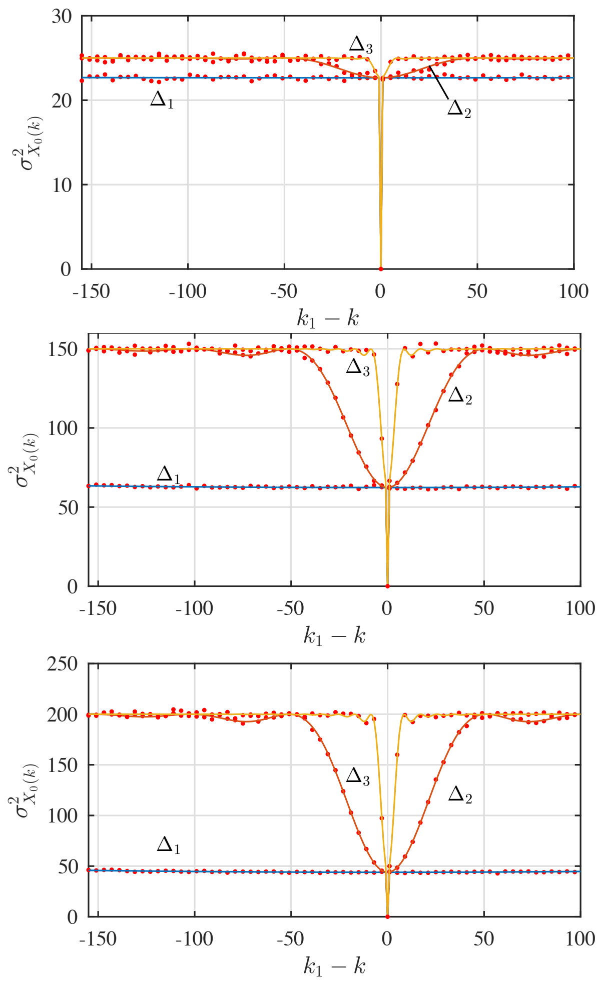

Fig. 3. Variance of the DFT coefficient as a function of $k_1 - k$ in the cases of a signal with: $M = 25$ available samples (top), $M = 150$ available samples (middle), and $M = 200$ available samples (bottom). Three values of Δ are considered: $\Delta_1 = 0.1, \Delta_2 = 5$, and $\Delta_3 = 30$. Lines represent theoretical values, whereas dots correspond to the numerical results.

V. Conclusions

The results for variances of nonuniformly sampled signal and a reduced set of samples are derived and verified. The results for a subset of uniformly sampled signals and randomly sampled signals follow as the special cases. These results will be used in our future work to define the reconstruction conditions and to calculate a threshold for one step matching pursuit reconstruction algorithms in ISAR. The obtained results will

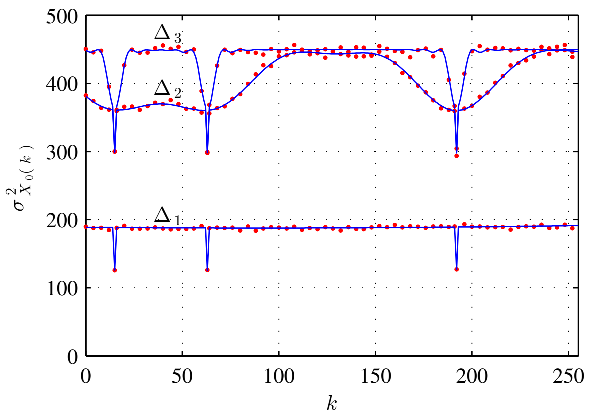

Fig. 4. Variance of the DFT coefficient as a function of k in the case of signal with three components with: $k_1 = 15$, $k_2 = 64$ and $k_3 = 192$ with $M = 150$ available samples. The results are presented for three considered values of Δ: $\Delta_1 = 0.1, \Delta_2 = 5$, and $\Delta_3 = 30$. Lines represent theoretical values, whereas dots correspond to the numerical results.

also be used to derive the error in the final, real data, ISAR signal reconstruction using a reduced set of samples when the sparsity condition is not satisfied. This will enable the analysis of the cases when both the signal samples and the transformation coefficients are off-grid.

References

[1] D. Donoho, "Compressed sensing," *IEEE Transactions on Information Theory*, vol. 52, no. 4, pp. 1289–1306, 2006.

[2] R. Baraniuk, "Compressive sensing," *IEEE Signal Processing Magazine*, vol. 24, no. 4, pp. 118–121, 2007.

[3] E. J. Candès and M. B. Wakin, "An introduction to compressive sampling," *IEEE Signal Processing Magazine*, vol. 25, no. 2, pp. 21–30, 2008.

[4] L. Zhang, M. Xing, C. W. Qiu J. Li, Z. Bao, "Achieving higher resolution ISAR imaging with limited pulses via compressed sampling," *IEEE Geoscience and Remote Sensing Letters*, Vol.6, No.3, 2009, pp.567–571

[5] J. H. G. Ender, "On compressive sensing applied to radar," *Signal Processing*, Vol. 90, No. 5, 2010, pp.1402-1414

[6] Y. S. Yoon, M. G. Amin "Compressed sensing technique for high-resolution radar imaging," *Proc. SPIE 6968, Signal Processing, Sensor Fusion, and Target Recognition XVII*, 69681A (April 17, 2008); doi:10.1117/12.777175;

[7] V.M. Patel, G.R. Easley, D. M. Healy Jr., R. Chellappa, "Compressed synthetic aperture radar," *IEEE Journal of Selected Topics in Signal Processing*, Vol.4, No.2, 2010, pp.244-254

[8] G. Zhao, Z. Wang, Q. Wang, G. Shi, F. Shen, "Robust ISAR imaging based on compressive sensing from noisy measurements," *Signal Processing*, Vol. 92, No. 1, 2012, pp.120-129

[9] X. C. Xie, Y. H. Zhang. "High-resolution imaging of moving train by ground-based radar with compressive sensing." *Electronics letters*, vol. 46, no. 7, 2010, pp.529-531.

[10] W. Qiu, E. Giusti, A. Bacci, M. Martorella, F. Berizzi, H. Z. Zhao, Q. Fu, "Compressive sensing for passive ISAR with DVB-T signal," *14th International Radar Symposium (IRS)*, June 2013, pp.113-118.

[11] W. Qiu, M. Martorella, F. Berizzi, "Interferometric ISAR imaging based on compressive sensing." *2nd International Workshop on Compressed Sensing Applied to Radar*, Sept. 2013, Bonn, Germany.

[12] L. Stanković, *Digital Signal Processing with Selected Topics*. CreateSpace Independent Publishing Platform, An Amazon.com Company, 2015.

[13] L. Stanković, I. Stanković, M. Daković, "Analysis of Noise and Nonsparsity in the ISAR Image Recovery from a Reduced Set of Data," *4th CoSeRa 2016*, 19-22 September, Aachen, Germany, 2016.

[14] H. Rauhut, "Stability results for random sampling of sparse trigonometric polynomials," *IEEE Transactions on Information Theory*, vol.54, no.12, pp.5661–5670, 2008.

[15] L. Stanković, "On the ISAR Image Analysis and Recovery with Unavailable or Heavily Corrupted Data," *IEEE Transactions on Aerospace and Electronic Systems*, Vol.51, July 2015.

[16] L. Stanković, S. Stanković, and M. G. Amin, "Missing samples analysis in signals for applications to L-estimation and compressive sensing," *Signal Processing*, vol. 94, pp. 401–408, 2014.

[17] E. Candes, J. Romberg and T. Tao. "Robust uncertainty principles: Exact signal reconstruction from highly incomplete frequency information," *IEEE Transactions on Information Theory*, vol. 52, pp. 489–509, 2006.

[18] L. Stanković, I. Stanković, and M. Daković, "Nonsparsity influence on the ISAR recovery from a reduced set of data," *IEEE Transactions on Aerospace and Electronic Systems*, vol. 52, no. 6, 2016.

[19] H. Hassanieh, P. Indyk, D. Katabi, and E. Price, "Simple and practical algorithm for sparse Fourier transform," in *Proceedings of the twenty-third annual ACM-SIAM symposium on Discrete Algorithms*. Society for Industrial and Applied Mathematics, pp. 1183–1194, 2012.

[20] K. D. Ba, P. Indyk, E. Price, and D. P. Woodruff, "Lower bounds for sparse recovery," in *Proceedings of the twenty-first annual ACM-SIAM symposium on Discrete Algorithms*. SIAM, pp. 1190–1197, 2010.

[21] L. Stanković, M. Daković, I. Stanković, S. Vujović, "On the Errors in Randomly Sampled Nonsparse Signals Reconstructed with a Sparsuty Assumption" *IEEE Geoscience and Remote Sensing Letters*, vol. 14, no. 12, pp. 2453 - 2456, December 2017.